Carderock Division
Naval Surface Warfare Center
Bethesda, MD 20084-5000

CARDEROCKDIV-SME-CR-17-92 January 1993
Ship Materials Engineering Department
Research and Development Report

J and CTOD Estimation Equations for Shallow Cracks in Single Edge Notch Bend Specimens

by
Mark T. Kirk, University of Illinois
Robert H. Dodds, Jr., University of Illinois

Under contract to
Naval Surface Warfare Center
Annapolis Detachment, Carderock Division
Code 2814
Annapolis, MD 21402-5067

Prepared for
Division of Engineering
Office of Nuclear Regulatory Research
U.S. Nuclear Regulatory Commission
Washington, DC 20555
NRC FIN B6290

CARDEROCKDIV-SME-CR-17-92 J and CTOD Estimation Equations for Shallow Cracks in Single Edge Notch Bend Specimens

NUREG/CR-5969
UILU-ENG-91-2013
CDNSWC/SME-CR-17-92

J AND CTOD ESTIMATION EQUATIONS FOR SHALLOW CRACKS IN SINGLE EDGE NOTCH BEND SPECIMENS

Mark T. Kirk
Robert H. Dodds, Jr.

Manuscript Completed: November 1992
Date Published–

Prepared for
U.S. Nuclear Regulatory Commission
Office Of Nuclear Regulatory Research
Division Of Engineering
Washington, Dc 20555

NRC FIN No. B6290

Prepared by
Naval Surface Warfare Center
Annapolis Detatchment, Carderock Division
Code 2814
Annapolis, Maryland 21402–5067

ABSTRACT

Fracture toughness values determined using shallow cracked single edge notch bend, SE(B), specimens of structural thickness are useful for structural integrity assessments. However, testing standards have not yet incorporated formulas that permit evaluation of J and CTOD for shallow cracks from experimentally measured quantities (i.e. load, crack mouth opening displacement (CMOD), and load line displacement (LLD)). Results from two dimensional plane strain finite–element analyses are used to develop J and CTOD estimation strategies appropriate for application to both shallow and deep crack SE(B) specimens. Crack depth to specimen width (a/W) ratios between 0.05 and 0.70 are modelled using Ramberg–Osgood strain hardening exponents (n) between 4 and 50. The estimation formulas divide J and CTOD into small scale yielding (SSY) and large scale yielding (LSY) components. For each case, the SSY component is determined by the linear elastic stress intensity factor, K_I. The formulas differ in evaluation of the LSY component. The techniques considered include: estimating J or CTOD from plastic work based on load line displacement ($A_{pl}|_{LLD}$), from plastic work based on crack mouth opening displacement ($A_{pl}|_{CMOD}$), and from the plastic component of crack mouth opening displacement ($CMOD_{pl}$). $A_{pl}|_{CMOD}$ provides the most accurate J estimation possible. The finite–element results for all conditions investigated fall within 9% of the following formula:

$$J = \frac{K^2(1-\nu^2)}{E} + \frac{\eta_{J-C}}{Bb} A_{pl}|_{CMOD} \quad ; \text{where} \quad \eta_{J-C} = 3.785 - 3.101\frac{a}{W} + 2.018\left(\frac{a}{W}\right)^2$$

The insensitivity of η_{J-C} to strain hardening permits J estimation for any material with equal accuracy. Further, estimating J from CMOD rather than LLD eliminates the need to measure LLD, thus simplifying the test procedure. Alternate, work based estimates for J and CTOD have equivalent accuracy to this formula; however the η coefficients in these equations depend on the strain hardening coefficient. CTOD estimates based on scalar proportionality of $CTOD_{lsy}$ and $CMOD_{pl}$ are highly inaccurate, especially for materials with considerable strain hardening, where errors up to 38% occur.

Contents

Section No. **Page**

Abstract iii

List of Figures vi

List of Tables vii

1. **Introduction** 1

2. **Approach** 1

3. ***J* and CTOD Estimation Procedures** 2
   - 3.1 Current Standards 2
   - 3.2 New Proposals 3

4. **Finite-Element Modelling** 4

5. **Results and Discussion** 6
   - 5.1 Perfectly Plastic and Finite Element Proportionality Coefficients 8
   - 5.2 *J* and CTOD Estimation Errors 8
   - 5.3 Recommended *J* and CTOD Estimation Procedures 12
     - 5.3.1 Requirements for Accurate Estimation 12
     - 5.3.2 *J* Estimation 13
     - 5.3.3 CTOD Estimation 14

6. **Summary and Conclusions** 15

7. **References** 16

Appendix: Summary of Coefficients for *J* and CTOD Estimation 17

LIST OF FIGURES

Figure No.		Page
1	Ramberg–Osgood stress strain curves used in the finite–element analysis.	4
2	Finite element model of the a/W=0.25 SE(B) specimen.	5
3	Variation of coefficients in J and CTOD estimation equations with a/W and n.	7
4	Variation of constraint factor (m) with a/W and n.	8
5	Comparison of limit solution and finite–element results for a/W=0.15, n=50.	9
6	Variation of J and CTOD with LLD and CMOD for a/W=0.15, n=5 SE(B).	10
7	J and CTOD estimation errors for a/W=0.15, n=5 SE(B).	10
8	Variation of coefficients in J and CTOD estimation errors with a/W and n.	11
9	Effect of strain hardening on the linearity of the $CTOD_{key}$ – $CMOD_{pl}$ relation for a/W=0.50.	12
10	Comparison of eqn. 5.3.2.1 to finite–element data.	13
11	Error associated with using η_{J-C} values from eqn. 5.3.2.1.	14
12	Relationship between strain hardening coefficient (n) and ultimate to yield ratio (R) for a Ramberg–Osgood material.	14

LIST OF TABLES

Table No.		Page
1	SE(B) specimens modelled.	2
2	Calculation of coefficients in J and CTOD estimation formulas.	6
A1	Variation of η_{pl} with a/W and n for J estimation by eqn. 3.1.1.	17
A2	Variation of η_{J-C} with a/W and n for J estimation by eqn. 3.2.2.	17
A3	Variation of m with a/W and n for CTOD estimation by eqns. 3.1.2, 3.2.1, 3.2.3, and 3.2.4.	17
A4	Variation of η_{C-L} with a/W and n for CTOD estimation by eqn. 3.2.1.	18
A5	Variation of η_{C-C} with a/W and n for CTOD estimation by eqn. 3.2.3.	18
A6	Variation of r_{pl} with a/W and n for CTOD estimation by eqn. 3.1.2.	18
A7	Variation of η_b with a/W and n for CTOD estimation by eqn. 3.2.4.	18

ADMINISTRATIVE INFORMATION

The work reported herein was funded under the Elastic-Plastic Fracture Mechanics of LWR Alloys Program at the Annapolis Detachment, Carderock Division, Naval Surface Warfare Center, Contract number N61533-92-R-0030. The Program is funded by the U.S. Nuclear Regulatory Commission under Interagency Agreement RES-78-104. The Technical Program monitor is Dr. S.N. Malik at the USNRC. Technical monitoring of the contract was performed by Mr. Richard E. Link (CDNSWC 2814).

1. INTRODUCTION

Standardized procedures for fracture toughness testing require both sufficient specimen thickness to insure predominantly plane strain conditions at the crack tip and a crack depth of at least half the specimen width [1–3]. Within certain limits on load level and crack growth, these restrictions insure the existence of very severe conditions for fracture as described by the Hutchinson Rice Rosengren (HRR) crack–tip fields [4,5]. These conditions make the applied driving force needed to initiate fracture in a laboratory specimen lower than the value needed to initiate fracture in common civil and marine structures where such severe geometric conditions are not present. As a consequence, structures often carry greater loads without failure than predicted from fracture toughness values measured using standardized procedures.

Both Sumpter [6] and Kirk and Dodds [7] achieved good agreement between the initiation fracture toughness of single edge notched bend, SE(B), specimens and structures containing part–through semi–elliptical surface cracks by matching thickness and crack depth between specimen and structure. These results demonstrate that toughness values determined from shallow cracked SE(B) specimens are appropriate for assessing the fracture integrity of structures. However, testing standards have not yet incorporated formulas permitting evaluation of J and CTOD for shallow cracks from experimental measurements (i.e. load, crack mouth opening displacement (CMOD), and load line displacement (LLD)). This investigation develops J and CTOD estimation procedures applicable for both shallow and deep crack fracture toughness testing for materials with a wide range of strain hardening characteristics.

2. APPROACH

Two dimensional, plane–strain finite–element analyses of SE(B) specimens are performed for crack depths from 0.05 to 0.70 a/W with Ramberg–Osgood strain hardening coefficients (n) between 4 and 50. Table 1 summarizes the conditions considered. The analyses provide load, CMOD, and LLD records to permit evaluation of coefficients relating J and CTOD to measurable quantities. The range of parameters considered in these analyses allows evaluation of the dependence of these coefficients on a/W and n. The estimation formulas divide J and CTOD into small scale yielding (SSY) and large scale yielding (LSY) components. In each formula, the SSY component is defined by the linear elastic stress intensity factor, K_I. The formulas differ only in the LSY component. Procedures to estimate the LSY component include:

1. J_{lsy} from plastic work (area under the load vs. LLD_{pl} curve, or $A_{pl}|_{LLD}$)
2. $CTOD_{lsy}$ as a fraction of $CMOD_{pl}$ using a rotation factor
3. $CTOD_{lsy}$ from plastic work (area under the load vs. LLD_{pl} curve, or $A_{pl}|_{LLD}$)
4. J_{lsy} and $CTOD_{lsy}$ from plastic work (area under the load vs. $CMOD_{pl}$ curve, or $A_{pl}|_{CMOD}$)

5. $CTOD_{ty}$ as a fraction of $CMOD_{pl}$ without the notion of a rotation factor

Existing standards employ the first two techniques [1–3]; the remainder are new proposals.

Table 1: SE(B) specimens modelled.				
	Ramberg–Osgood Strain Hardening Coefficient (n)			
a/W	4	5	10	50
0.05	✓	✓	✓	✓
0.15	✓	✓	✓	✓
0.25	✓	✓	✓	✓
0.50	✓	✓	✓	✓
0.70	✓	✓	✓	✓

3. *J* AND CTOD ESTIMATION PROCEDURES

3.1 Current Standards

Existing test standards for *J* and CTOD [1–3] employ the following estimation formulas:

$$J = \frac{K^2(1-\nu^2)}{E} + \frac{\eta_{pl}}{Bb} A_{pl}|_{LLD} \tag{3.1.1}$$

$$CTOD = \frac{K^2(1-\nu^2)}{m\sigma_{flow}E} + \frac{r_{pl}\, bCMOD_{pl}}{r_{pl}\, b + a} \tag{3.1.2}$$

where

K	linear elastic stress intensity factor
ν	Poisson's ratio
η_{pl}	plastic eta factor
B	specimen thickness
b	remaining ligament, $W - a$
$A_{pl}\|_{LLD}$	area under the load vs. LLD_{pl} curve
m	constraint factor
σ_{flow}	flow stress, average of yield and ultimate[1]
r_{pl}	plastic rotation factor
$CMOD_{pl}$	plastic component of CMOD

Values of η_{pl}, m, and r_{pl} are well established for perfectly plastic materials based on closed form solutions. For deeply cracked specimens ($a/W \geq 0.5$), current test standards use $\eta_{pl} = 2$, $m = 2$, and $r_{pl} = 0.44$ Sumpter [8] and Wu., et al. [9] have proposed the following relations to account for crack depth less than 0.5 a/W:

1. ASTM E1290 and BS 5762 both use yield stress in the CTOD estimation equation. In this investigation, flow stress is used instead.

$$\eta_{pl} = 0.32 + 12\frac{a}{W} - 49.5\left(\frac{a}{W}\right)^2 + 99.8\left(\frac{a}{W}\right)^3 \quad \text{for } a/W < 0.282 \tag{3.1.3}$$

$$\eta_{pl} = 2.0 \quad \text{for } a/W \geq 0.282$$

$$r_{pl} = 0.5 + 0.42\frac{a}{W} - 4\left(\frac{a}{W}\right)^2 \quad \text{for } a/W < 0.172$$

$$r_{pl} = 0.463 - 0.04\frac{a}{W} \quad \text{for } a/W \geq 0.172 \tag{3.1.4}$$

Sumpter derived the η_{pl} equation from limit analyses of the SE(B), while Wu, Cotterell, and Mai used a slip line field analysis to determine the variation of r_{pl} with *a/W*. Material strain hardening alters the deformation characteristics of the specimen, thereby altering η_{pl}, m, and r_{pl}. Existing procedures neglect any influence of strain hardening.

3.2 New Proposals

The estimation formulas presented in Section 3.1 have received the greatest attention as the coefficients relating *J* and CTOD to experimental measurements are amenable to closed form solution, at least in the non–hardening limit. For hardening materials, closed form solution is not possible, therefore either experimental techniques [10] or finite–element analyses [11] are used to provide data from which η_{pl}, m, and r_{pl} are calculated. Quantities other than $CMOD_{pl}$ and $A_{pl}|_{LLD}$ measured during a test can also be related to *J* or CTOD, if the proper proportionality coefficient is known. The following are some alternatives:

1. Estimate $CTOD_{lsy}$ from plastic work ($A_{pl}|_{LLD}$):

$$CTOD = \frac{K^2(1-\nu^2)}{m\sigma_{flow}E} + \frac{\eta_{C-L}}{Bb\sigma_{flow}}A_{pl}|_{LLD} \tag{3.2.1}$$

   This formula is analogous to eqn. 3.1.1 for *J* testing

2. Use plastic work defined by the area under the load vs. $CMOD_{pl}$ curve ($A_{pl}|_{CMOD}$) to estimate either J_{lsy} or $CTOD_{lsy}$:

$$J = \frac{K^2(1-\nu^2)}{E} + \frac{\eta_{J-C}}{Bb}A_{pl}|_{CMOD} \tag{3.2.2}$$

$$CTOD = \frac{K^2(1-\nu^2)}{m\sigma_{flow}E} + \frac{\eta_{C-C}}{Bb\sigma_{flow}}A_{pl}|_{CMOD} \tag{3.2.3}$$

   This technique eliminates the need for LLD measurement, which simplifies *J* testing.

3. Express $CTOD_{lsy}$ as a fraction of $CMOD_{pl}$:

$$CTOD = \frac{K^2(1-\nu^2)}{m\sigma_{flow}E} + \eta_\delta CMOD_{pl} \tag{3.2.4}$$

   Eqn. 3.2.4 and 3.1.2 are functionally the same, thus η_δ and r_{pl} are related:

$$\eta_\delta = \frac{r_{pl}\,b}{r_{pl}\,b + a} \tag{3.2.5}$$

   Sorem [11] found r_{pl} to be extremely sensitive to the CTOD–CMOD relationship for shallow cracks. This estimation procedure was proposed to circumvent this sensitivity. The validity of this approach is based on the observed, nearly linear dependence of $CTOD_{lsy}$ on $CMOD_{pl}$ in finite–element solutions.

In this investigation, finite–element analyses provide data from which η_{pl}, m, r_{pl}, η_{C-L}, η_{J-C}, η_{C-C}, and η_{δ} are calculated.

4. FINITE–ELEMENT MODELLING

Two–dimensional, plane strain finite–element analyses of SE(B) specimens are performed using conventional small strain theory. The analyses are conducted using the POLO–FINITE analysis software [12] on an engineering workstation.

Uniaxial stress strain behavior is described using the Ramberg–Osgood model

$$\frac{\varepsilon}{\varepsilon_o} = \frac{\sigma}{\sigma_o} + \alpha\left(\frac{\sigma}{\sigma_o}\right)^n \tag{4.1}$$

where σ_o is the reference stress (0.2% offset yield stress when $\alpha = 1$), $\varepsilon_o = \sigma_o/E$ is the reference strain, $\alpha = 1$, and n is the strain hardening coefficient. Strain hardening coefficients of 4, 5, 10, and 50 model materials ranging from highly strain hardening to nearly elastic – perfectly plastic. Figure 1 illustrates these stress – strain curves.

J_2 deformation plasticity theory (nonlinear elasticity) describes the multi–axial material model. Total strains and stresses are related by

$$\varepsilon_{ij} = \left[\frac{1+\nu}{E} + \frac{3\alpha\varepsilon_o}{2\sigma_o}\left(\frac{\sigma_e}{\sigma_o}\right)^{n-1}\right]s_{ij} + \frac{1-2\nu}{3E}\sigma_{kk}\delta_{ij}, \quad \sigma_e = \sqrt{\frac{3}{2}s_{ij}s_{ij}} \tag{4.2}$$

where s_{ij} is the stress deviator, σ_e is the Mises equivalent tensile stress, σ_{kk} is the trace of the stress tensor, and δ_{ij} is the Kronecker delta.

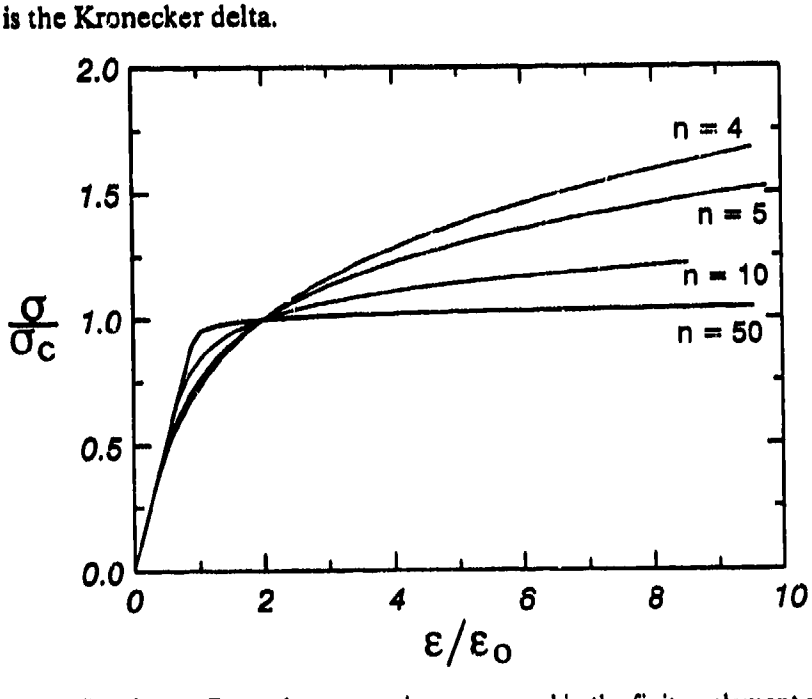

Figure 1: Ramberg–Osgood stress strain curves used in the finite–element analysis.

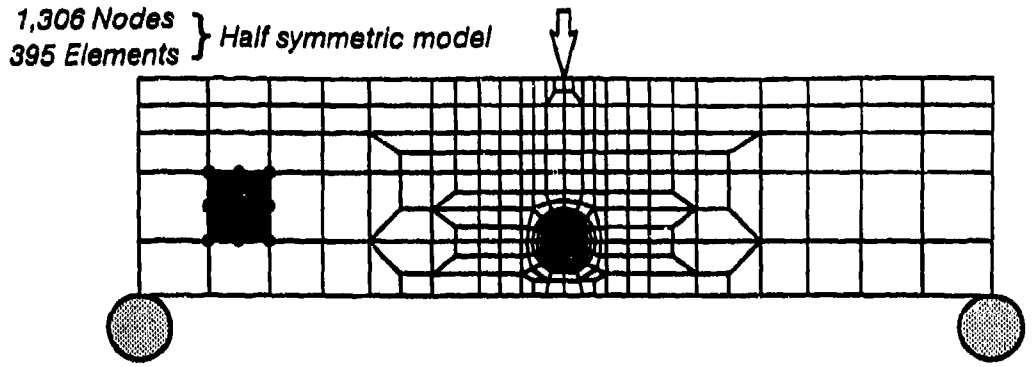

Figure 2: Finite–element model of the a/W=0.25 SE(B) specimen.

Finite–element models are constructed for a/W ratios of 0.05, 0.15, 0.25, 0.50, and 0.70. The SE(B) specimens have standard proportions; the unsupported span is four times the specimen width. Symmetry of both geometry and loading permit use of a half–symmetric model. Each model contains approximately 400 elements and 1300 nodes; the a/W = 0.25 model is shown in Figure 2. Eight–noded, plane–strain isoparametric elements are used throughout. Reduced (2 x 2) Gaussian integration is used to eliminate locking of the elements under incompressible plastic deformation. The same half–circular core of elements surrounds the crack tip in all models. This core consists of eight, equally sized wedges (22.5° each) of elements in the θ direction. Each wedge contains 30 quadrilateral elements; the radial dimension decreases geometrically with decreasing element distance to the crack tip. The eight crack–tip elements are collapsed into wedges with the initially coincident nodes left unconstrained to permit development of crack–tip blunting deformations. The side nodes of these elements are retained at the mid–point position. This modelling produces a $1/r$ strain singularity appropriate in the limit of perfect plasticity. Crack–tip element sizes range from 0.2% to 0.02% of the crack length depending on the a/W modelled.

Load is uniformly distributed over two small elements and applied at the center of the compression face of the specimen to eliminate the local singularity effects caused by a concentrated nodal load. Load is increased in 30 to 50 variably sized steps until the CTOD reaches 5% of the crack length. Strict convergence criteria at each step insure convergence of calculated stresses and strains to the third significant figure. Two to three full Newton iterations at each load step are required to satisfy this criteria. As deformation plasticity is strain path independent, converged solutions are load step size invariant.

The J–integral is computed at each load step using a domain integral method [13,14]. J values calculated over domains adjacent to and remote from the crack tip are within 0.003% of each other, as expected for deformation plasticity. CTOD is computed from the blunted shape of the crack flanks using the $\pm$ 45° intercept procedure. LLD is taken as the relative displacement in the loading direction of a node on the symmetry plane located approximately $0.4b$ ahead of the crack tip and of a node located above the support. This procedure eliminates the effect of spuriously high displacements in

Table 2: Calculation of coefficients in J and CTOD estimation formulas.			
Eqn.	Coefficient	X	Y
3.1.1	η_{pl}	$\frac{A_{pl}\|_{LLD}}{Bb}$	J_{pl}
3.2.2	η_{J-C}	$\frac{A_{pl}\|_{CMOD}}{Bb}$	J_{pl}
3.1.2 3.2.3 3.2.1 3.2.4	m	$\delta\sigma_{flow}$ †	J
3.2.1	η_{C-L}	$\frac{A_{pl}\|_{LLD}}{Bb\sigma_{flow}}$	δ_{pl}
3.2.3	η_{C-C}	$\frac{A_{pl}\|_{CMOD}}{Bb\sigma_{flow}}$	δ_{pl}
3.1.2	r_{pl}	$CMOD_{pl}$ *	δ_{pl}
3.2.4	η_{δ}	$CMOD_{pl}$	δ_{pl}
*: μ is the slope of this line, $r_{pl} = \frac{\mu a}{b(1-\mu)}$ †: δ = CTOD			

the vicinity of both the load and support points. The η, m, and r_{pl} coefficients are determined from these results by calculating the slope of the quantities indicated in Table 2 at each load step. Slope calculation is initiated with data from the final three load steps. Data from earlier load steps are included in this calculation until the linear correlation coefficient (r) falls below 0.999. This procedure eliminates data from the first few load steps, which are predominantly elastic, and therefore not expected to provide reliable relationships between plastic quantities.

5. RESULTS AND DISCUSSION

The variation of the η, m, and r_{pl} coefficients with a/W and n determined from the finite–element results is summarized in Figures 3–4, and in the Appendix. Solutions for non–hardening materials, where available, are indicated on the figures. Each coefficient shows considerable variation with crack depth. The variation with material strain hardening is also a common feature of all coefficients except η_{J-C} which relates J_{lsy} to $A_{pl}|_{CMOD}$. η_{J-C} is essentially independent of n for $a/W \geq 0.15$. The remainder of this section examines the differences between perfectly plastic and finite–element solutions, and the errors associated with each estimation procedure. Finally, recommendations of J and CTOD estimation formulas for use in fracture testing of SE(B) specimens are made.

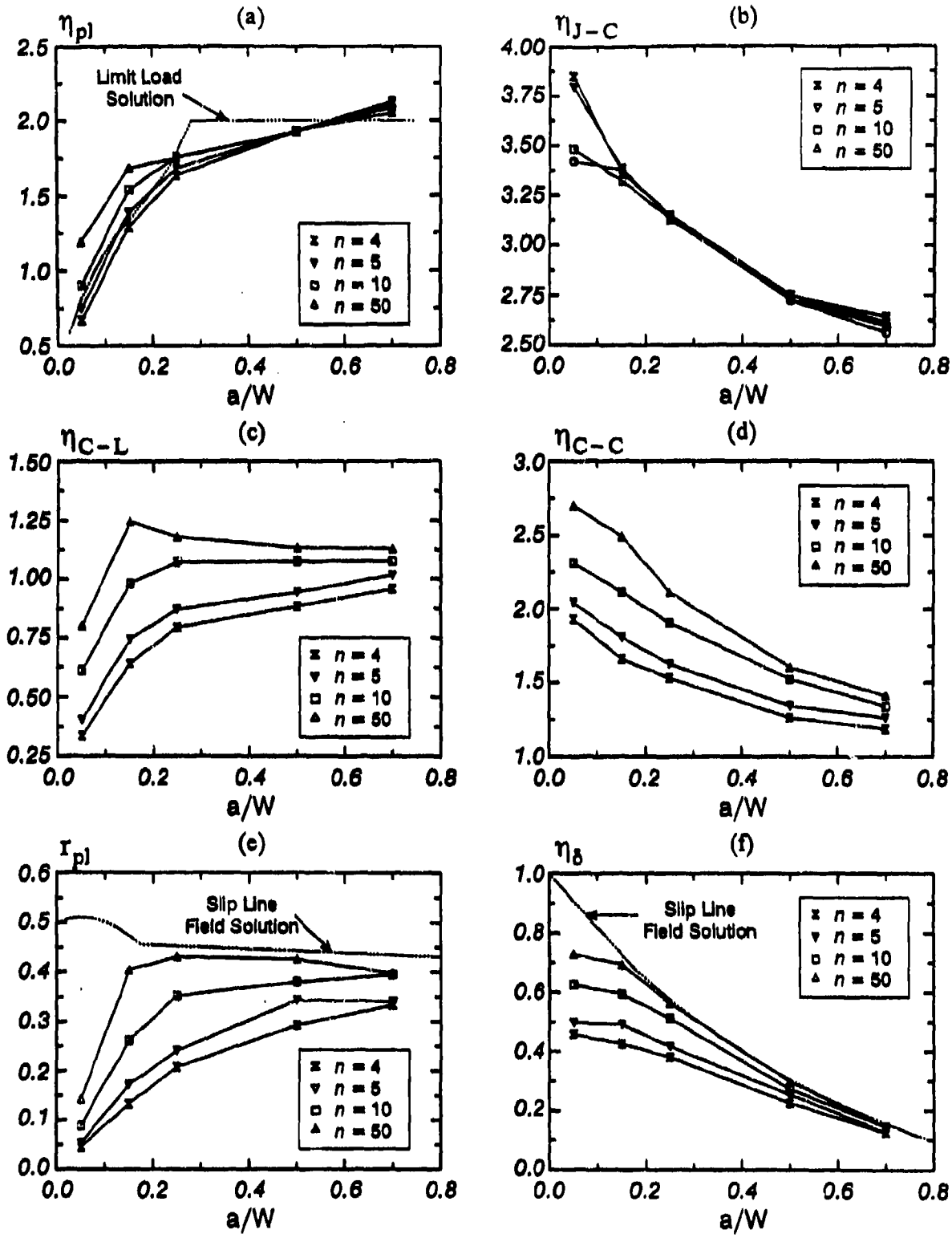

Figure 3: Variation of coefficients in J and CTOD estimation equations with a/W and n. (a) eqn. 3.1.1, (b) eqn. 3.2.2, (c) eqn. 3.2.1, (d) eqn. 3.2.3, (e) eqn. 3.1.2, (f) eqn.3.2.4.

5.1 *Perfectly Plastic and Finite Element Proportionality Coefficients*

The variation of both r_{pl} and η_δ with a/W for a low strain hardening material (Figure 3 e–f) agrees well with the slip line field solution of Wu, et al. [9] above a/W=0.15. However, at smaller a/W the elastically dominated response, ignored in the slip line field solution, causes a deviation between the slip line field and finite–element r_{pl} and η_δ values.

The variation of η_{pl} with a/W determined by finite–element analysis has a different functional form than determined by Sumpter [8] using a limit load solution (Figure 3a). The limit load derivation employs the following approximation for plastic work:

$$U_{PL} = P_{LIM} \cdot LLD_{PL} \tag{5.1.1}$$

where

$$P_{LIM} = \frac{\zeta B W^2 \sigma_{flow}}{S}$$

$$\zeta = 1 - 0.33\frac{a}{W} - 6\left(\frac{a}{W}\right)^2 + 15.5\left(\frac{a}{W}\right)^3 - 19.8\left(\frac{a}{W}\right)^4$$

S = unsupported bend span

Thus, the accuracy of η_{pl} values determined by limit analysis depends on the equivalence of plastic work calculated by eqn. 5.1.1 and the actual plastic work (area under a load vs. LLD_{pl} diagram) for a strain hardening material. This equivalence is not achieved even for the low strain hardening n=50 material, as illustrated in Figure 5.

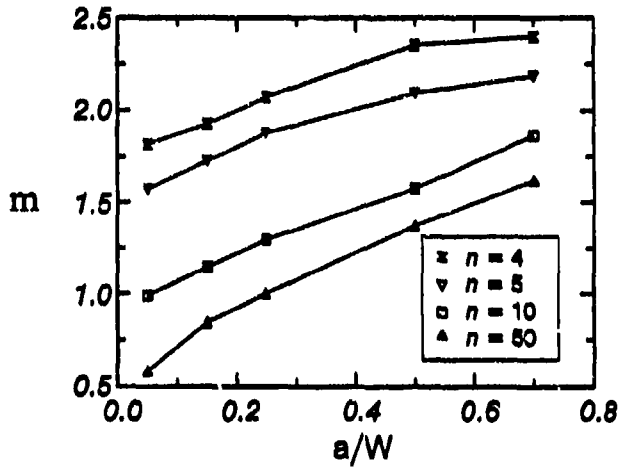

Figure 4: Variation of constraint factor (m) with a/W and n.

5.2 *J and* CTOD *Estimation Errors*

Figure 6 illustrates the variation of J and CTOD with LLD and CMOD for an a/W=0.15, n=5 SE(B) determined by finite–element analysis. This dependence of fracture parameters on measurable quantities is contrasted with that predicted by the J and CTOD estimation procedures using η and m coefficients calculated from the finite–element results. Work–based J and CTOD estimates (eqns.

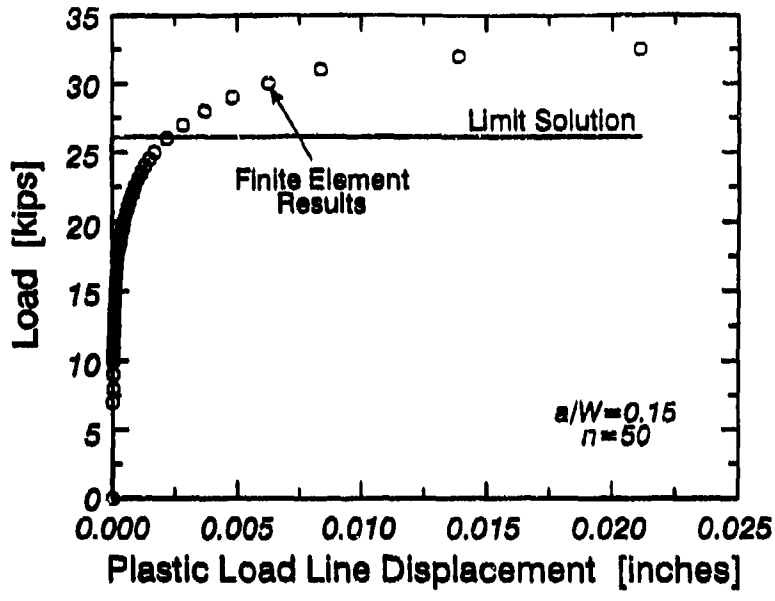

Figure 5: Comparison of limit solution and finite–element results for a/W=0.15, n=50.

3.1.1, 3.2.1, 3.2.2, and 3.2.3) match the finite–element results much more closely than do formulas that calculate $CTOD_{lsy}$ as a fraction of $CMOD_{pl}$ (eqns. 3.1.2 and 3.2.4). Figure 7 shows J and CTOD estimation errors, more clearly illustrating the differences between the estimation procedures. To evaluate the effects of both a/W and n on estimation accuracy, the following error measure is defined:

$$\overline{ERR} = \sum_{i=1}^{N} |E_i FP^{fe}_i| \Big/ \sum_{i=1}^{N} FP^{fe}_i \qquad (5.2.1)$$

where

$$E_i = \frac{FP^{est}_i - FP^{fe}_i}{FP^{fe}_i} 100 \quad \text{percent error at load step } i$$

N total number of load steps
FP^{est}_i estimated J or CTOD at load step i
FP^{fe}_i J or CTOD at load step i from finite–element analysis

For an a/W=0.15 / n=5 SE(B), the $\overline{ERR}$ value for CTOD estimation using r_{pl}, eqn. 3.1.2, is 21%. Comparison of this value with the data in Figure 7demonstrates that $\overline{ERR}$ is a root mean square error measure.

The variation of $\overline{ERR}$ with a/W and n for the six estimation procedures is shown in Figure 8. Errors associated with work–based J and CTOD estimates (work calculated from CMOD) are below 5% for all a/W and n. If work is instead calculated from LLD, J and CTOD estimation errors are also generally below 5%, with the exception of shallow cracks in a very low strain hardening material (a/W=0.05, n=50). However, equations that express $CTOD_{lsy}$ as a fraction of $CMOD_{pl}$ are inaccurate for all a/W ($\overline{ERR}$ > 17%) in highly strain hardening materials ($n \leq 5$). As the maximum estimation er-

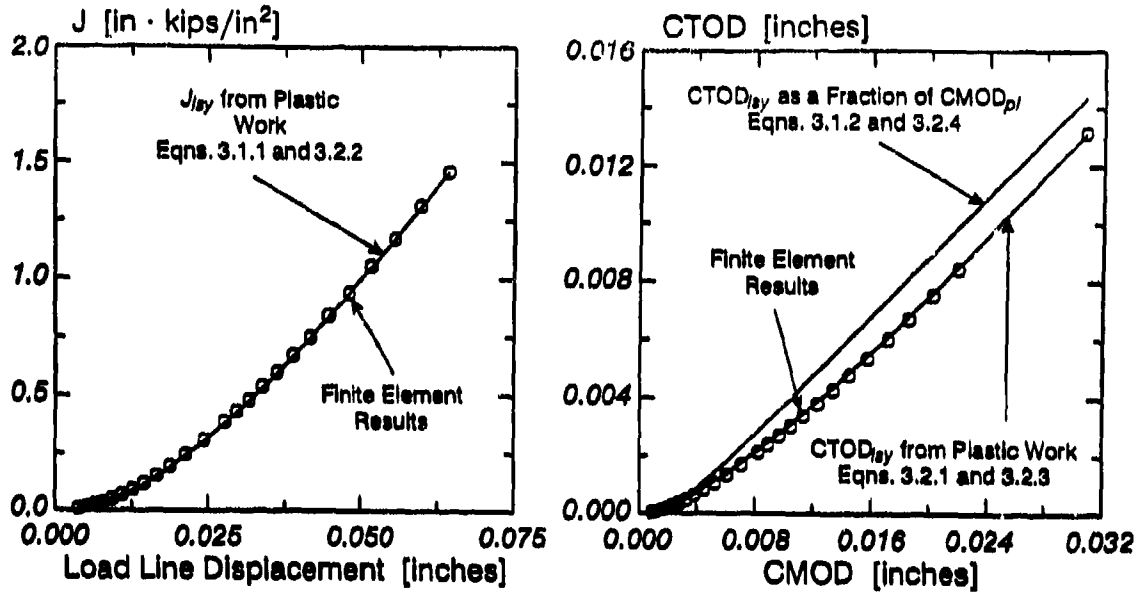

Figure 6: Variation of J and CTOD with LLD and CMOD for a/W=0.15, n=5 SE(B).

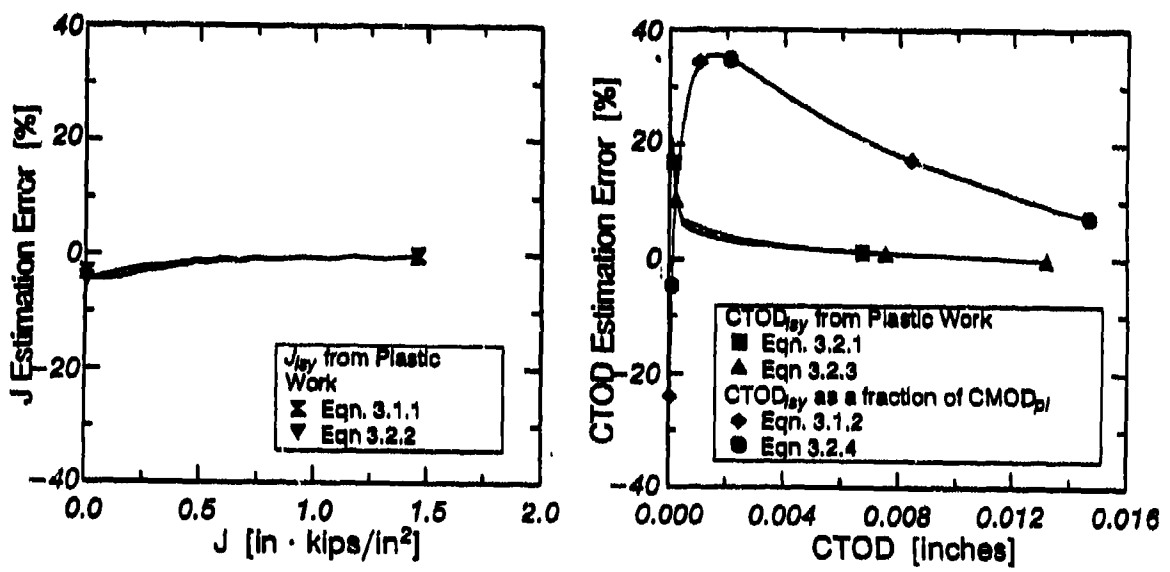

Figure 7: J and CTOD estimation errors for a/W=0.15, n=5 SE(B).

ror can exceed $\overline{ERR}$ by up to a factor of 2 (Figure 7), $\overline{ERR}$ values above 17% are clearly excessive. Accuracy improves ($\overline{ERR}$<12%) for materials with less strain hardening (n ≥ 10). However, these estimates have accuracy comparable to work–based CTOD estimates only for deep cracks in essentially non–hardening materials. Thus, the validity of assumptions made in deriving the various es-

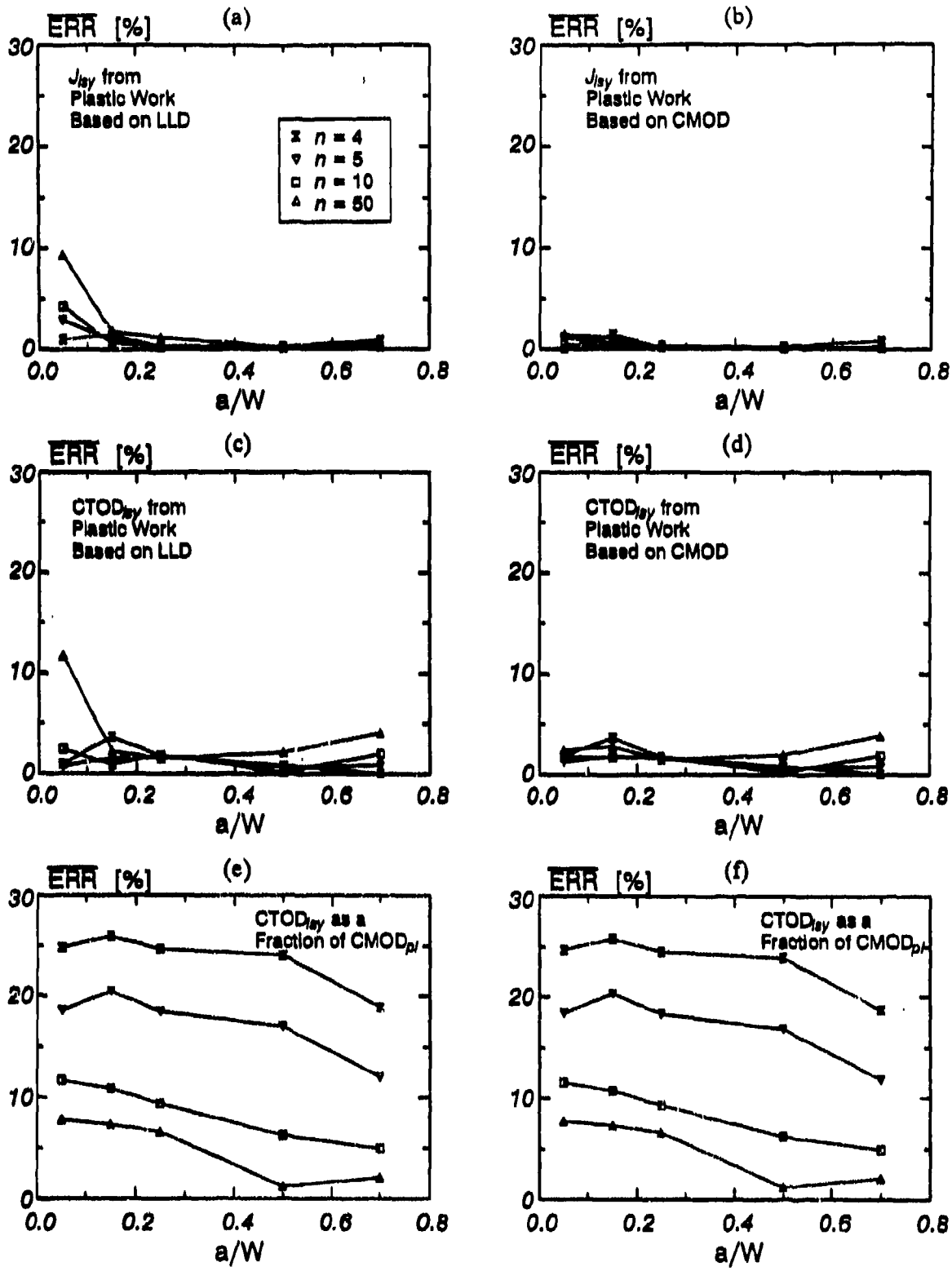

Figure 8: Variation of J and CTOD estimation errors with a/W and n. Symbols represent the same conditions in each figure. (a) eqn. 3.1.1, (b) eqn. 3.2.2, (c) eqn. 3.2.1, (d) eqn. 3.2.3, (e) eqn. 3.1.2, (f) eqn. 3.2.4.

timation procedures directly affects their accuracy. J and CTOD estimation from plastic work is achieved by partitioning total work into *SSY* and *LSY* components. Additive separation is exact because, for a linear elastic body, $K^2(1 - \nu)/E$ is the elastic strain energy. Conversely, the linear relation between $CTOD_{lsy}$ and $CMOD_{pl}$ assumed in eqns. 3.1.2 and 3.2.4 cannot exist (exactly) for any body with an elastic component that varies with load (i.e. for any amount of strain hardening). Strain hardening strongly influences the linearity of the $CTOD_{lsy}$ – $CMOD_{pl}$ relationship, as illustrated in Figure 9. Thus, eqns. 3.1.2 and 3.2.4 work best for minimally strain hardening materials.

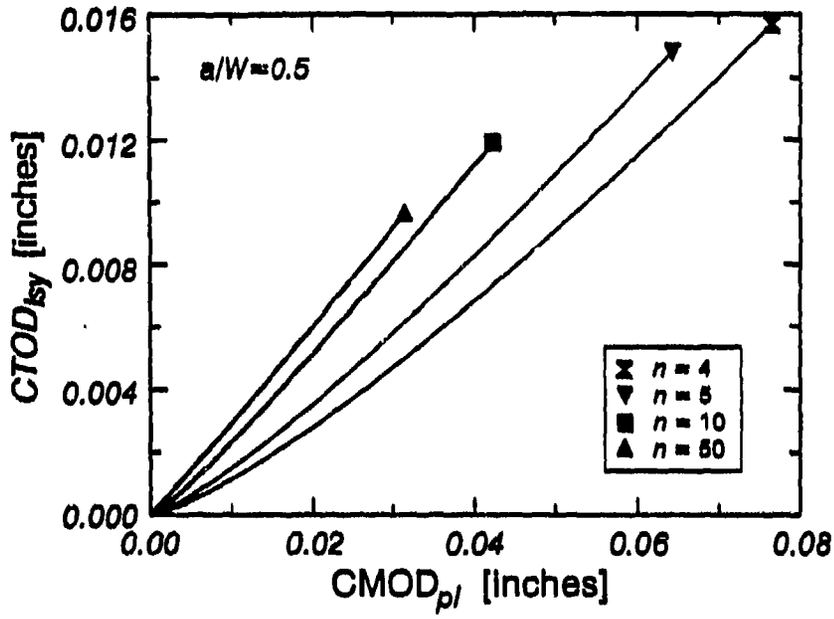

Figure 9: Effect of strain hardening on the linearity of the $CTOD_{lsy}$ – $CMOD_{pl}$ relation for a/W=0.50.

5.3 *Recommended J and* CTOD *Estimation Procedures*

5.3.1 *Requirements for Accurate Estimation*

The formulas used to evaluate fracture parameters from experimental data should not introduce substantial errors into the J and CTOD estimates. This need for accuracy favors estimating J_{lsy} and $CTOD_{lsy}$ from plastic work. Even though estimation of the *LSY* component from plastic work requires numerical integration of experimental data, this seems warranted to reduce errors by up to five–fold (compare Figure 8d to Figure 8f). In addition to using inherently accurate formulas, selecting η, m, and r_{pl} coefficients corresponding to a specific a/W and material should not be a potential error source. In view of the ambiguity attendant to fitting experimental stress–strain data with a power law curve, insensitivity of η, m, and r_{pl} to material strain hardening would be extremely advantageous.

5.3.2 J Estimation

The only procedure that meets both of the aforementioned requirements is J estimation from plastic work based on CMOD. By fitting the data in Figure 3b, the variation of η_{J-C} with a/W is expressed as follows:

$$\eta_{J-C} = 3.785 - 3.101\frac{a}{W} + 2.018\left(\frac{a}{W}\right)^2 \quad \text{for all } n, \quad 0.05 \le \frac{a}{W} \le 0.70 \qquad (5.3.2.1)$$

Figure 10 shows this fit together with the η_{J-C} data. The use of η_{J-C} values from eqn. 5.3.2.1 produces estimation errors of at most 9%, and generally much less, as illustrated in Figure 11. In situations where fracture toughness in terms of a critical J value is desired, estimation using eqns. 3.2.2 and 5.3.2.1 is clearly superior to estimating J from plastic work based on LLD, where η_{pl} depends on material strain hardening coefficient. Further, estimating J from CMOD rather than LLD eliminates the need to measure LLD, which simplifies the test procedure.

Despite the clear advantages of estimating J from plastic work based on CMOD, estimation based on LLD may be necessary for very shallow cracks due to experimental complexities associated with clip gage attachment [15]. If J estimation using LLD is unavoidable, η_{pl} can be indexed less ambiguously to the ratio of the ultimate strength to the yield strength than to the strain hardening coefficient. The ultimate tensile strength for a Ramberg–Osgood material is obtained by solving for the tensile instability point, converting true stress to engineering stress, and taking the ratio of this value with 0.2% offset yield stress. This calculation gives:

The variation of $1/n$ with R calculated from eqn. 5.3.2.2 is shown in Figure 12. This figure, along with the information in Table A1, is used to determine the appropriate η_{pl} value for the experimental conditions of interest based on data from a simple tensile test.

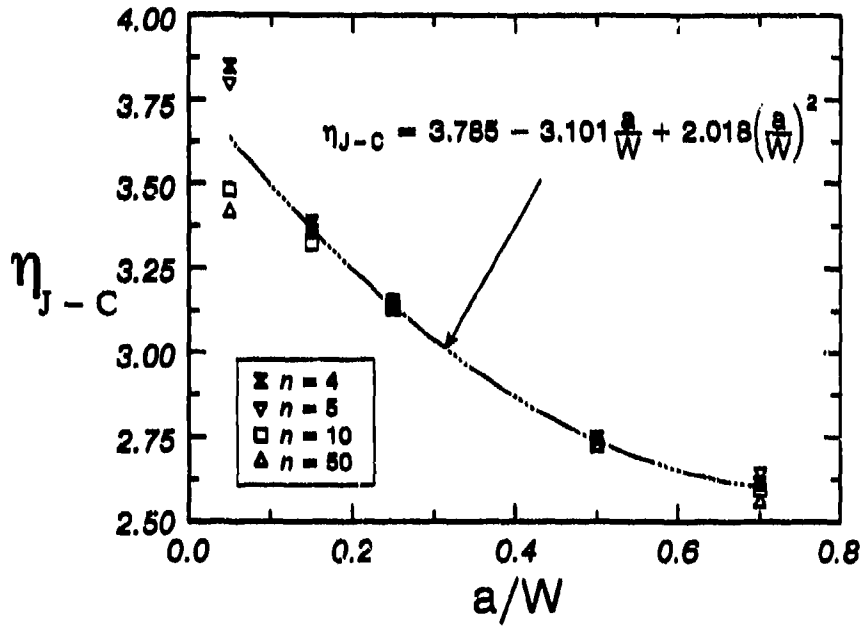

Figure 10: Comparison of eqn. 5.3.2.1 to finite–element data.

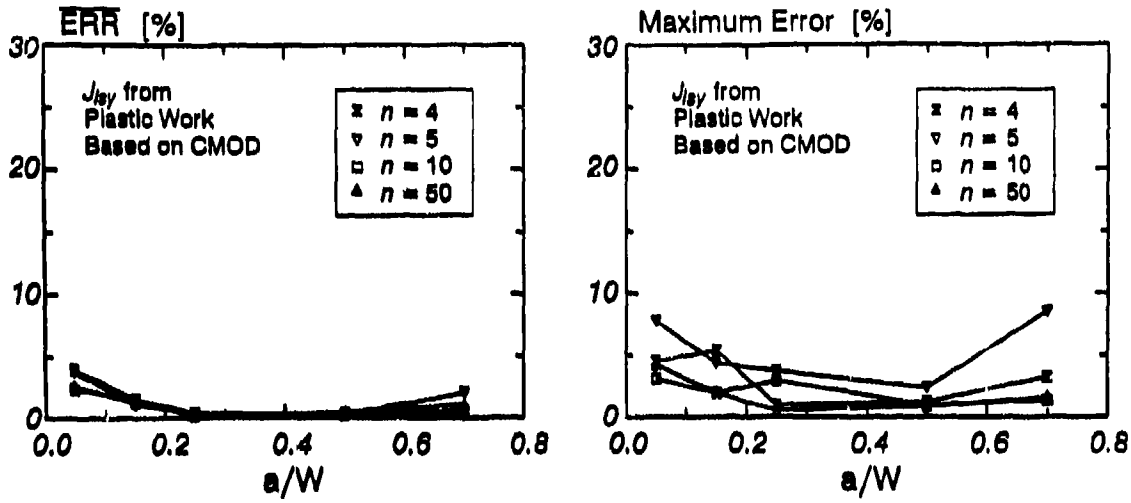

Figure 11: Error associated with using η_{J-C} values from eqn. 5.3.2.1.

$$R = \frac{\sigma_u}{\sigma_o} = \left(\frac{1}{0.002n}\right)^{\frac{1}{n}} / \exp\left(\frac{1}{n}\right) \qquad (5.3.2.2)$$

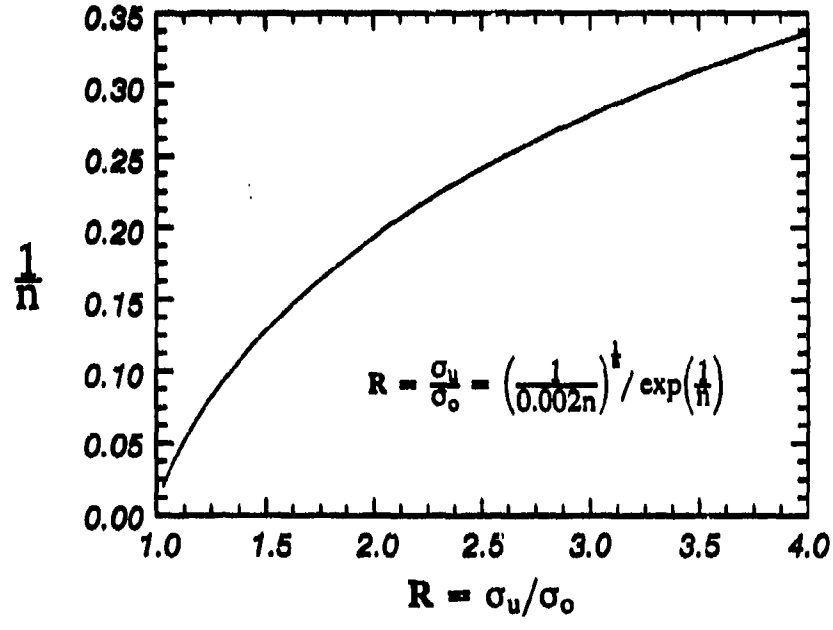

Figure 12: Relationship between strain hardening coefficient (n) and ultimate to yield ratio (R) for a Ramberg–Osgood material.

5.3.3 CTOD *Estimation*

As noted previously, CTOD estimation from plastic work is considerably more accurate than CTOD estimation directly from $CMOD_{pl}$. Use of eqn. 3.2.1 or 3.2.3 is therefore preferred to eqn. 3.1.2 or

3.2.4. However, the η, m, and r_{pl} coefficients in all of these equations depend strongly on n. The strain hardening coefficient is estimated from R as described in section 5.3.1. Appropriate m and η_{C-L} or η_{C-C} values for the experimental conditions of interest are then determined from Tables A3, A4, and A5, respectively.

6. SUMMARY AND CONCLUSIONS

Results from two-dimensional, plane strain finite-element analyses are used to develop J and CTOD estimation strategies appropriate for application in both shallow and deep crack SE(B) specimens. Crack depth to specimen width (a/W) ratios between 0.05 and 0.70 are modelled using Ramberg-Osgood strain hardening exponents (n) between 4 and 50. The estimation formulas divide J and CTOD into small scale yielding (SSY) and large scale yielding (LSY) components. For each case, the SSY component is determined by the linear elastic stress intensity factor, K_I. The formulas differ in evaluation of the LSY component. The techniques considered include: estimating J or CTOD from plastic work based on load line displacement ($A_{pl}|_{LLD}$), from plastic work based on crack mouth opening displacement ($A_{pl}|_{CMOD}$), and from the plastic component of crack mouth opening displacement ($CMOD_{pl}$). $A_{pl}|_{CMOD}$ provides the most accurate J estimation possible. The finite-element results for all conditions investigated fall within 9% of the following formula:

$$J = \frac{K^2(1-\nu^2)}{E} + \frac{\eta_{J-C}}{Bb} A_{pl}|_{CMOD} \quad ; \text{where} \quad \eta_{J-C} = 3.785 - 3.101\frac{a}{W} + 2.018\left(\frac{a}{W}\right)^2$$

The insensitivity of η_{J-C} to strain hardening permits J estimation for any material with equal accuracy. Further, estimating J from CMOD rather than LLD eliminates the need to measure LLD, thus simplifying the test procedure. Alternate, work based estimates for J and CTOD have equivalent accuracy to this formula; however the η coefficients in these equations depend on the strain hardening coefficient. CTOD estimates based on scalar proportionality of $CTOD_{tip}$ and $CMOD_{pl}$ are highly inaccurate, especially for materials with considerable strain hardening, where errors up to 38% occur.

7. REFERENCES

[1] ASTM Standard Test Method for J_{Ic}, A Measure of Fracture Toughness, E813–89.

[2] ASTM Standard Test Method for Crack–Tip Opening Displacement (CTOD) Fracture Toughness Measurement, E1290–89.

[3] BS 5762: 1979, "Methods for Crack Tip Opening Displacement (*COD*) Testing," British Standards Institution, London, 1979.

[4] Hutchinson, J.W., "Singular Behavior at the End of a Tensile Crack in a Hardening Material," *Journal of Mechanics and Physics of Solids*, Vol. 16, pp. 13–31, 1968.

[5] Rice, J.R., and Rosengren, G.F., "Plane Strain Deformation Near a Crack Tip in a Power–Law Hardening Material," *Journal of Mechanics and Physics of Solids*, Vol. 16, pp. 1–12, 1968.

[6] Sumpter, J.D.G., "Prediction of Critical Crack Size in Plastically Strained Welded Panels," *Nonlinear Fracture Mechanics: Volume II – Elastic–Plastic Fracture, ASTM STP 995*, J.D. Landes, A. Saxena, and J.G. Merkle, eds., American Society for Testing and Materials, pp. 415–432, 1989.

[7] Kirk, M.T., and Dodds, R.H., "An Analytical and Experimental Comparison of J_I Values for Shallow Through and Part Through Surface Cracks," *Engineering Fracture Mechanics*, Vol. 39, No. 3, pp. 535–551, 1991.

[8] Sumpter, J.D.G., "J_c Determination for Shallow Notch Welded Bend Specimens," *Fatigue and Fracture of Engineering Materials and Structures*, Vol. 10, No. 6, pp. 479–493, 1987.

[9] Wu, S.X., Cotterell, B., and Mai, Y.W., "Slip Line Field Solutions for Three–Point Notch–Bend Specimen," *International Journal of Fracture*, Vol. 37, pp. 13–29, 1988.

[10] Wu, S.X., "Plastic Rotational Factor and *J–COD* Relationship of Three Point Bend Specimen," *Engineering Fracture Mechanics*, Vol. 18, No. 1, pp. 83–95, 1983.

[11] Sorem, W.A., Dodds, R.H., and Rolfe, S.T., "Effects of Crack Depth on Elastic Plastic Fracture Toughness," *International Journal of Fracture*, Vol. 47, pp. 105–126, 1991.

[12] Dodds, R.H., and Lopez, L.A., "Software Virtual Machines for Development of finite–element Systems," *International Journal for Engineering with Computers*, Vol. 13, pp. 18–26, 1985.

[13] Li, F.Z., Shih, C.F., and Needleman, A., "A Comparison of Methods for Calculating Energy Release Rates," *Engineering Fracture Mechanics*, Vol. 21, pp. 405–421, 1985.

[14] Shih, C.F., Moran, B., and Nakamura, T., "Energy Release Rate Along a Three–Dimensional Crack Front in a Thermally Stressed Body," *International Journal of Fracture*, Vol. 30, pp. 79–102, 1986.

[15] Theiss, T.J., and Bryson, J.R., "Influence of Crack Depth on Fracture Toughness of Reactor Pressure Vessel Steel," to appear in the ASTM STP resulting from the *Symposium on Constraint Effects in Fracture*, held May 8–9 1991, Indianapolis, Indiana.

APPENDIX
SUMMARY OF COEFFICIENTS FOR *J* AND CTOD ESTIMATION

Table A1: Variation of η_{pl} with a/W and n for J estimation by eqn. 3.1.1.				
	Ramberg–Osgood Strain Hardening Coefficient (n)			
a/W	4	5	10	50
0.05	0.670	0.746	0.901	1.192
0.15	1.295	1.393	1.542	1.687
0.25	1.639	1.686	1.763	1.753
0.50	1.924	1.930	1.924	1.927
0.70	2.109	2.130	2.086	2.052

Table A2: Variation of η_{J-C} with a/W and n for J estimation by eqn. 3.2.2.				
	Ramberg–Osgood Strain Hardening Coefficient (n)			
a/W	4	5	10	50
0.05	3.848	3.793	3.482	3.420
0.15	3.359	3.385	3.322	3.376
0.25	3.152	3.138	3.130	3.137
0.50	2.748	2.749	2.728	2.723
0.70	2.613	2.641	2.595	2.562

Table A3: Variation of m with a/W and n for CTOD estimation by eqns. 3.1.2, 3.2.1, 3.2.3, and 3.2.4.				
	Ramberg–Osgood Strain Hardening Coefficient (n)			
a/W	4	5	10	50
0.05	1.908	1.786	1.496	1.291
0.15	1.963	1.863	1.573	1.423
0.25	2.036	1.938	1.648	1.501
0.50	2.177	2.047	1.788	1.687
0.70	2.200	2.093	1.932	1.810

Table A4: Variation of η_{C-L} with a/W and n for CTOD estimation by eqn. 3.2.1.				
	Ramberg–Osgood Strain Hardening Coefficient (n)			
a/W	4	5	10	50
0.05	0.335	0.402	0.611	0.800
0.15	0.640	0.743	0.982	1.245
0.25	0.795	0.872	1.073	1.121
0.50	0.885	0.944	1.076	1.[illegible]
0.70	0.959	1.018	1.078	1.131

Table A5: Variation of η_{C-C} with a/W and n for CTOD estimation by eqn. 3.2.3.				
	Ramberg–Osgood Strain Hardening Coefficient (n)			
a/W	4	5	10	50
0.05	1.929	2.043	2.310	2.701
0.15	1.659	1.806	2.115	2.493
0.25	1.530	1.624	1.904	2.112
0.50	1.263	1.344	1.525	1.605
0.70	1.187	1.262	1.341	1.412

Table A6: Variation of η_{pl} with a/W and n for CTOD estimation by eqn. 3.1.2.				
	Ramberg–Osgood Strain Hardening Coefficient (n)			
a/W	4	5	10	50
0.05	0.045	0.053	0.089	0.142
0.15	0.132	0.171	0.261	0.404
0.25	0.207	0.240	0.352	0.431
0.50	0.292	0.343	0.380	0.426
0.70	0.333	0.341	0.395	0.398

Table A7: Variation of η_b with a/W and n for CTOD estimation by eqn. 3.2.4.				
	Ramberg–Osgood Strain Hardening Coefficient (n)			
a/W	4	5	10	50
0.05	0.459	0.499	0.627	0.729
0.15	0.427	0.492	0.595	0.695
0.25	0.382	0.418	0.512	0.563
0.50	0.226	0.255	0.274	0.299
0.70	0.125	0.127	0.145	0.146

INITIAL DISTRIBUTION

OUTSIDE CENTER

Copies

1 DDRE/Lib

1 CNO/OP 098T

2 OCNR
- 1 1132 (Rajapakse)
- 1 1132 (Vasudivan)
- 1 0225
- 1 432S
- 1 Lib

1 NAVPGSCOL

1 USNROTCU
NAVADMINU MIT

2 NRL
- 1 Code 6380
- 1 Code 6384

8 NAVSEA
- 1 (SEA05M)
- 1 (SEA05M2)
- 1 (SEA05P)
- 1 (SEA05P1)
- 1 (SEA05P2)
- 1 (SEA05P3)
- 2 (SEA08S)

2 DTIC

5 USNRC
- 1 (M. Mayfield)
- 2 (Dr. S.N. Malik)
- 1 (A. Hiser)
- 1 (Dr. E.M. Hackett)

1 DOE, Oak Ridge

2 NIST, Boulder
- 1 Lib
- 1 (J. Berger)

4 NIST, Washington
- 1 Lib
- 1 (R. Fields)
- 1 (R. DeWitt)
- 1 (J.T. Fong)

1 Brown Univ.
- 1 (Dr. C.F. Shih)

1 Univ. of Illinois
- 1 (Dr. R.H. Dodds, Jr.)

1 Texas A&M Univ.
- 1 (Dr. T.L. Anderson)

2 NASA/Langley
- 1 Lib
- 1 (Dr. J.C. Newman)

1 Hibbit, Karlsson and Sorenson, Inc.

CENTER DISTRIBUTION

Copies

1	0115
1	17
1	1702
1	1703
1	172
2	172.4
1	173
2	173.3
1	174.3
1	175
1	175.1
1	28
1	2801
5	281
1	2812
1	2813
12	2814
5	2814 (R. Link)
1	2815
1	3421
1	3422

NAVSEES

1	043
1	043.1
1	043C
1	045
1	045B

REPORT DOCUMENTATION PAGE

Form Approved

1. AGENCY USE ONLY (Leave blank) | 2. REPORT DATE | 3. REPORT TYPE AND DATES COVERED: Final

4. TITLE AND SUBTITLE

J AND CTOD ESTIMATION EQUATIONS FOR SHALLOW CRACKS IN SINGLE EDGE NOTCH BEND SPECIMENS

5. FUNDING NUMBERS

C: N61533-92-R-0030

WU: 93-1-2814-554

6. AUTHOR(S)

MARK T. KIRK AND ROBERT H. DODDS, JR.

7. PERFORMING ORGANIZATION NAME(S) AND ADDRESS(ES)

NAVAL SURFACE WARFARE CENTER
CARDEROCK DIVISION
ANNAPOLIS DETACHMENT
ANNAPOLIS, MD 21402

8. PERFORMING ORGANIZATION REPORT NUMBER

CDNSWC/SME-CR-17-92

9. SPONSORING/MONITORING AGENCY NAME(S) AND ADDRESS(ES)

US NUCLEAR REGULATORY COMMISSION
MATERIALS ENGINEERING BRANCH
NL/S 217C
WASHINGTON, DC 20555

10. SPONSORING/MONITORING AGENCY REPORT NUMBER

NUREG/CR-5969

11. SUPPLEMENTARY NOTES

12a. DISTRIBUTION/AVAILABILITY STATEMENT

Approved for public release; distribution is unlimited

12b. DISTRIBUTION CODE

13. ABSTRACT (Maximum 200 words)

Results from two dimensional plane strain finite-element analyses are used to develop J and CTOD estimation strategies appropriate for application to both shallow and deep crack SE(B) specimens. Crack depth to specimen width (a/W) ratios between 0.05 and 0.70 are modelled using Ramberg-Osgood strain hardening exponents (n) between 4 and 50. The estimation formulas divide J and CTOD into small scale yielding (SSY) and large scale yielding (LSY) components. For each case, the SSY components is determined by the linear elastic stress intensity factor, K_I. The formulas differ in evaluation of the LSY component. The techniques considered include: estimating J or CTOD from plastic work based on load line displacement ($A_{pl}|_{LLD}$), from plastic work based on crack mouth opening displacement ($A_{pl}|_{CMOD_{pl}}$), and from the plastic component of crack mouth opening displacement ($CMOD_{pl}$). $A_{pl}CMOD$ provides the most accurate J estimation possible. CTOD estimates based on scalar proportionality of $CTOD_{lsy}$ and $CMOD_{pl}$ are highly inaccurate, especially for materials with considerable strain hardening, where errors up to 38% occur.

14. SUBJECT TERMS

KEYWORDS: J-integral, crack-tip opening displacement, fracture toughners, finite element method, shallow crack, structural integrity eta factor.

15. NUMBER OF PAGES

16. PRICE CODE

17. SECURITY CLASSIFICATION OF REPORT	18. SECURITY CLASSIFICATION OF THIS PAGE	19. SECURITY CLASSIFICATION OF ABSTRACT	20. LIMITATION OF ABSTRACT
unclassified	unclassified	unclassified	UL